Atherosclerosis 354 (2022) 41–52

Contents lists available at ScienceDirect

Atherosclerosis

journal homepage: www.elsevier.com/locate/atherosclerosis

De novo DNA methylation induced by circulating extracellular vesicles from acute coronary syndrome patients

Concetta Schiano [a,b,c,*,1], Carolina Balbi [b,c,d,1], Jacopo Burrello [c,e], Antonio Ruocco [f], Teresa Infante [a], Carmela Fiorito [g], Stefano Panella [c,e], Lucio Barile [c,e], Ciro Mauro [f], Giuseppe Vassalli [b,c,d,2], Claudio Napoli [a,h,2]

[a] *Department of Advanced Medical and Surgical Sciences (DAMSS), University of Campania Luigi Vanvitelli, Naples, Italy*
[b] *Cellular and Molecular Cardiology lab Istituto Cardiocentro Ticino-EOC, Lugano, Switzerland*
[c] *Laboratories for Translation Research, EOC, Bellinzona, Switzerland*
[d] *Center for Molecular Cardiology, Zurich, Switzerland*
[e] *Cardiovascular Theranostics, Istituto Cardiocentro Ticino-EOC, Lugano, Switzerland*
[f] *Unit of Cardiovascular Diseases and Arrhythmias, Antonio Cardarelli Hospital, Naples, Italy*
[g] *Azienda Universitaria Policlinico (AOU), Naples, Italy*
[h] *Division of Clinical Immunology, Immunohematology, Transfusion Medicine and Transplant Immunology (SIMT), Regional Reference Laboratory of Transplant Immunology (LIT), Azienda Universitaria Policlinico (AOU), Naples, Italy*

ARTICLE INFO

Keywords:
Extracellular vesicles
Exosome
Epigenetics
DNA methyltransferase
Heart
Acute coronary syndrome

ABSTRACT

Background and aims: DNA methylation is associated with gene silencing, but its clinical role in cardiovascular diseases (CVDs) remains to be elucidated. We hypothesized that extracellular vesicles (EVs) may carry epigenetic changes, showing themselves as a potentially valuable non-invasive diagnostic liquid biopsy. We isolated and characterized circulating EVs of acute coronary syndrome (ACS) patients and assessed their role on DNA methylation in epigenetic modifications.

Methods: EVs were recovered from plasma of 19 ACS patients and 50 healthy subjects (HS). Flow cytometry, qRT-PCR, and Western blot (WB) were performed to evaluate both intra-vesicular and intra-cellular signals. ShinyGO, PANTHER, and STRING tools were used to perform GO and PPI network analyses.

Results: ACS-derived EVs showed increased levels of DNA methyltransferases (DNMTs) ($p < 0.001$) and Ten-eleven translocation (TET) genes reduction. Specifically, *de novo* methylation transcripts, as DNMT3A and DNMT3B, were significantly increased in plasma ACS-EVs. DNA methylation analysis on PBMCs from healthy donors treated with HS- and ACS-derived EVs showed an important role of DNMTs carried by EVs. PPI network analysis evidenced that ACS-EVs induced changes in PBMC methylome. In the most enriched subnetwork, the *hub* gene *SRC* was connected to *NOTCH1, FOXO3, CDC42, IKBKG, RXRA, DGKG, BAIAP2* genes that were showed to have many molecular effects on various cell types into onset of several CVDs. Modulation in gene expression after ACS-EVs treatment was confirmed for *SRC, NOTCH1, FOXO3, RXRA, DGKG* and *BAIAP2* ($p < 0.05$).

Conclusions: Our data showed an important role for ACS-derived EVs in gene expression modulation through *de novo* DNA methylation signals, and modulating signalling pathways in target cells.

1. Introduction

Acute coronary syndrome (ACS) is associated with high mortality and includes acute myocardial infarction (AMI) and unstable angina, which are both life- and health-threatening [1]. The World Health Organization (WHO) has estimated that the number of people with

* Corresponding author. University of Campania "Luigi Vanvitelli" Department of Advanced Medical and Surgical Sciences Department of Advanced Medical and Surgical Sciences (DAMSS), University of Campania L. Vanvitelli, Naples, Italy, Cellular and Molecular Cardiology lab Istituto Cardiocentro Ticino-EOC, Lugano, Switzerland Piazza Miraglia 2, 80138, Naples, Italy.
E-mail address: concetta.schiano@unicampania.it (C. Schiano).
[1] These authors contributed equally to this work.
[2] These authors share the senior authorship.

https://doi.org/10.1016/j.atherosclerosis.2022.06.1026
Received 8 April 2022; Received in revised form 25 June 2022; Accepted 29 June 2022
Available online 6 July 2022

cardiovascular disease (CVDs) could increase to about 23 million by 2030. In the last years, the interest in the role of nano-sized vesicles, commonly referred to as extracellular vesicles (EVs), is significantly increased in both physiological and pathological conditions. The EVs, as defined by the International Society of Extracellular Vesicles (ISEV) include exosomes, microvesicles (MVs) and apoptotic bodies [2]. Recent evidence has suggested a key role for EVs in CVDs [3]. EVs are lipid bilayer membrane vesicles that carry a variety of molecules such as proteins, lipids and nucleic acids. Circulating EVs are being largely studied since they could represent an ideal sample for "liquid biopsy" as their content reflects changes in the condition of the cell of origin. However, to date, it is not clear whether they carry "damage" or "repairing" signals. *In vitro* experiments report that all cell types, included cardiomyocytes, endothelial cells (ECs) and fibroblasts, release EVs [4,5]. It is now known that the content of EVs depends in part on the secretion stimuli. Indeed, in hypoxic conditions, stem cells derived EVs were able to enhance they content of both angiogenic and survival factors [6,7]. Furthermore, it has been shown that EVs derived from mesenchymal cardiac progenitor cells (CPCs), in a model of myocardial infarction (MI), can inhibit cardiomyocyte apoptosis, induce cardiac repair and regeneration and promote angiogenesis [8–11]. For the above reasons, CPCs has emerged as one of the most promising types of progenitor cells for cardiac regeneration and repair [12,13]. Although there is expanding interest in the role of EVs in CVDs, their use as biomarkers in clinical research is still very limited [14–16]. Epigenetic mutations, including aberrant DNA methylation, histone modifications, and RNA silencing, are found in several human diseases, such as CVDs [17]. In the eukaryotic genome, the principal methylation marks are often found in CpG dinucleotides, presenting as C5-methylcytosine (5 mC), generated by writers DNA methyltransferases (DNMTs) enzymes. These factors, through a covalent reaction, form an intermediate complex between the enzyme and the substrate base [18]. The human genome encodes five DNMTs: DNMT1, DNMT2, DNMT3A, DNMT3B and DNMT3L. The main members of the family include DNMT1, DNMT3A and DNMT3B, which are canonical cytosine-5 DNMTs that catalyse the addition of methylation marks to genomic DNA. The expression of DNMTs in different tissues is associated with aberrant methylation [19], occurring in the gene promoters and acting as a transcriptional mechanism silencer switch [20]. On the other hand, DNA demethylation is intrinsically linked to DNA repair. DNA demethylation is either a passive mechanism or an active process regulated by erasers ten-eleven translocation (TET) enzymes. TETs catalyse the oxidation of 5-methylcytosine to allow the insertion of unmethylated cytosine in the deleted base site and the induction of base excision repair [21]. Emerging evidence suggests interplay between DNMTs, TETs, active DNA instability and the DNA damage response [22]. Several studies reported that epigenetic marks are associated with the pathogenesis of coronary heart disease (CHD) and significantly contribute to atherosclerosis progression [23–31]. The aim of this study was to elucidate the potential role of circulating EVs in ACS patients in the modulation of gene expression through epigenetic-sensitive mechanisms.

2. Materials and methods

For the expanded methods section please refer to Supplementary material.

2.1. Sample collection – EV characterization

In accordance with the principles outlined in the Declaration of Helsinki and with prior informed consent, a peripheral venous blood sample was taken from subjects with ACS in the acute condition enrolled in the DIANA clinical study (NCT04371809) according to Prot. No. 683 of 10/10/2018 [21]. The blood sampling was obtained at presentation to the emergency department, within about 5 h after the onset of chest pain in ACS patients. The bio-clinical characteristics of all ACS patients are reported in Supplementary Table 1.

EVs isolation and nanoparticle tracking analysis (NTA) were used to confirm EVs isolation and purification. Flow cytometry, quantitative Real Time PCR (qRT-PCR) and Western blot analysis were performed to evaluate intra-vesicular and intra-cellular signals. DNA integrity was checked on 1% agarose gel (Supplementary Figure 1). The oligonucleotide sequences are shown in Supplementary Table 2.

2.2. Functional analyses and protein-protein interaction network analysis

PBMCs DNA methylome data have been deposited in the ArrayExpress database at EMBL-EBI (www.ebi.ac.uk/arrayexpress) under accession number E-MTAB-11641. Enrichment analysis, gene ontology (GO) and pathway analysis of DMR-related genes (DMG) located at different regions were done with the ShinyGO v0.75 application (http://bioinformatics.sdstate.edu/go/) [32] and PANTHER (Protein Analysis Through Evolutionary Relationships, http://www.pantherdb.org) (version 16.0) [33] for comparison of PBMC results after ACS- *vs* HS-EV treatments.

The protein-protein interaction (PPI) network was constructed by Search Tool for the Retrieval Interacting Genes (STRING) v9.1 (https://string-db.org) to build four unique methylome protein-protein interaction (PPI) sub-networks in ACS-EV treatment by mapping both hyper- and hypo-methylated DMGs, independently of their genomic localization [34].

2.3. Data and statistical analysis

Kolmogorov-Smirnov test was used to assess variable distribution. Normally distributed variables were expressed as mean ± standard deviation (SD) and analyzed by Student *t*-test for independent variables. Non-normally distributed variables were expressed as median and interquartile range and analyzed with Mann-Whitney non-parametric test. Ordinal variables were expressed as absolute number and percentage and analyzed using chi-square test, or Fisher test, as appropriated. Correlations between gene expression data and patient characteristics were assessed by Spearman Rho test. *p*-values less than 0.05 were considered significant. IBM SPSS Statistics 26 (IBM, New York, USA) was used for statistical analyses. Results are shown as mean ± standard error of mean (SEM) from >3 independent experiments. Statistical analyses of differences between 3 groups were performed by one-way ANOVA followed by *post-hoc* Tukey's multiple tests, and those of differences between 2 groups were performed using unpaired *t*-test with Prism Version 9 GraphPad Software. Statistical significance was defined as $p < 0.05$.

3. Results

3.1. Baseline characteristics

Our study population included a total number of 69 subjects (19 were ACS patients, 50 HS). The clinical characteristics of ACS patients are shown in Supplementary Table 1. Ninety percent of the subjects included in the study were male (17). Among 19 ACS patients enrolled in this study, 68.4% (13) showed ST-segment elevation myocardial infarction (STEMI) and 31.6% non-ST-segment elevation myocardial infarction (NSTEMI) (6). STEMI patients had higher cardiac Troponin I (ng/L) (50.9 ± 57.0 *vs* 4.3 ± 5.9) ($p < 0.05$) and CK-MB (U/L) (1371.3 ± 1264.2 *vs* 331.2 ± 271.2) ($p < 0.05$) at the time of blood collection within 5 h of onset of chest pain, and they were younger (age 62 ± 11 *vs* 68 ± 12 years, $p > 0.05$) than NSTEMI patients (6). In contrast, patients with NSTEMI had hypertension (100.0% *vs* 76.9%) and a family history of coronary heart disease (83.3% *vs* 53.8%, $p < 0.05$) more often than STEMI patients.

3.2. EVs isolation and characterization

EVs obtained from HS and ACS plasma were isolated by ultracentrifuge and characterized using NTA and Western blot analysis. After EVs isolation, NTA showed no differences in the number and size of vesicles (mean and modal values) from both groups (Fig. 1A). This result could derive from the heterogeneity of the pathological cohort, since it included STEMI and NSTEMI, and from the time of blood sampling. Indeed, we have previously reported that a significant increase in the number and size of circulating EVs is observed in STEMI patients only within 2 h of chest pain onset [35]. Western blot analysis for exosomal markers, such as ALIX, TSG101 and CD81 confirm the presence of small EV in the preparation, with no differences between HS and ACS groups (Fig. 1B) [35]. Statistically significant decrease of APOB48 positivity, compared to the total plasma, validated the quality of the isolation method.

3.3. DNMTs/TETs cargo of EVs

In order to understand whether EVs can induce key epigenetic changes in ACS patients, we focused on their cargo. It is known that EVs contain a rich load of different RNA fragments with specialized functions however, the transfer of potential bio-epigenetic molecules from circulating EVs, remains largely unknown. RNA content isolated from ACS- and HS-EVs showed no differences between the two groups, as reported in Fig. 2A. The RNA amount from ACS-EVs was 13.2 ± 2.6 ng/μl *vs* 15.4 ± 2.3 ng/μl from HS-EVs. Moreover, we tested whether DNMTs/TETs, which are conserved epigenetic regulators of gene expression, could be transported by the ACS-EVs. We found that DNMT1, DNMT3A, and DNMT3B mRNA were significantly increased in plasma ACS-EVs. Specifically, DNMT1, DNMT3A and DNMT3B transcripts showed a fold change (FC) of 99.88 ($p < 0.05$), 103.80 ($p < 0.05$) and 74.12 ($p < 0.05$) *vs* HS-EVs, respectively (Fig. 2B). Among the 3 different TETs genes (*TET1, TET2*, and *TET3*) only TET1 mRNA was found altered in EVs, showing a slight, although not significant, decrease in ACS-EVs compared to HS-EVs (Fig. 2B).

The transfer of RNA from EVs and cell target was evaluated using a species-specific strategy. Rat cardiac fibroblasts were treated using human EVs and RealTime PCR (RT-PCR) with specific human primers was used to assess DNMT1, DNMT3A and DNMT3B levels transferred from circulating human EVs. As shown in Fig. 2C, EVs were efficiently able to transfer their RNA cargo to the target cells. DNA methylation is a critical epigenetic regulator in humans. In our previous study, we found a different methylation pathway between PBMCs isolated from HS or ACS patients [21]. Here, in order to evaluate the role of ACS-derived EVs on DNA methylation, we treated PBMCs from healthy donors with both ACS- and HS-derived EVs. After 24 h of treatment, we found no difference in the percentage of the PBMC population measured by flow cytometry analysis (Fig. 3A and B). To understand whether EVs could induce epigenetic-sensitive changes in the treated cells, we validated all genes that were altered in ACS- *vs* HS-PBMCs by RT-PCR analysis [23]. In particular, the *ABCA1* gene, which is most directly involved in cholesterol transport, showed a significant overexpression after ACS-EVs treatment (Fig. 3C). ABCA1 is indeed a gene known to be altered in CHD as previously reported from our laboratory [36]. On the other hand, genes that were indirectly involved in the cholesterol pathway, according to previous work, showed an increase for *NFATC1* and *PDGFA*, although not significant, while *TCF7, PRKCB* and *PRKCZ* showed a reduced relative gene expression (Supplementary Figure 2).

3.4. Methylome analysis of EVs treated PBMCs

To better investigate the role of EVs in triggering epigenetic modification, we analyzed EVs treated PBMCs isolated from HS using reduced representation bisulfite sequencing (RRBS). In order to compare PBMCs methylome, dmCpG analysis was performed. Specifically, we considered PBMCs samples incubated with ACS-EVs, HS-EVs and untreated PBMCs quantifying the amount of dmCpG sites after comparisons. After the exclusion step of dmCpGs without the gene symbol annotation, called "NA" (about 17%), we found that all dmCpGs were 920, of which 170 and 750 were hyper- and hypo-methylated, respectively for ACS-EVs *vs* HS-EVs (Supplementary Table 3) and 3005, of which 1248 and 1757 were hyper- and hypo-methylated, respectively for ACS-EVs *vs* untreated PBMCs comparisons (Supplementary Table 4). Of note, dmCpG number is much higher when we consider the DNA methylome of untreated PBMCs. The significant dmCpGs, which exhibited greater and lesser methylation differences were: ring finger protein 166 (*RNF166*) and Transmembrane Protein 177 (*TMEM177)*, showing a q value of 3.86E-08 and 8.58E-03, respectively for hyper-methylated genes; whereas cyclin D3 (*CCND3*) and protocadherin gamma subfamily B, 3 (*PCDHGB3)*, displayed a q value of 4.41E-09 and 1.37E-02, respectively for hypo-methylated genes. According to the genomic annotation, the most abundant dmCpGs were intergenic (81), among these 36% were hypo- and 13% were hyper-methylated (Fig. 4A). Then, when dmCpGs were annotated with respect to gene regions, we observed that DNA methylation dynamics were rather concentrated among CpG islands located in the non-coding intronic regions (74 hypo- and 23 hyper-methylated) for ACS-EVs *vs* HS-EVs comparison (Fig. 4B). When we considered only the gene symbol annotation, PBMCs after ACS-EVs treatment showed approximately 75% (124) hypo- and approximately 25% (41) hyper-methylated CpGs comparing to HS-EVs. Finally, to characterize the most significant specific annotated genes, which were differentially methylated by ACS-EVs, we listed all genes that were mapped based on their distance from the established differential methylation positions (DMPs), in according with q value (Supplementary Table 5). In general, we observed that the number of hypo-methylated was greater than that of hyper-methylated DMGs both for ACS-EVs *vs* HS-EVs (114 *vs* 28) and ACS-EVs *vs* untreated cells (227 *vs* 310) (Supplementary Table 5 and Supplementary Table 6). In Supplementary Tables 7 and 8, we reported the top 10 hyper- and hypo-methylated related genes that showed a significant methylation difference in the promoter regions.

3.5. Gene functional enrichment analysis

To illustrate the biological classification of DMGs, GO term enrichment analysis was carried out using ShinyGO and PANTHER applications. Three categories of GO terms including the biological process (BP), cellular component (CC), and molecular function (MF) results are presented in Fig. 5A–D. As reported in Supplementary Table 9, results suggested that changes in BP of the top significant DMGs were significantly enriched in signaling pathway as "Homophilic cell adhesion via plasma membrane adhesion molecules", "Nervous system development", "Anoikis", and "Mitral valve formation" (FDR<0.05). On the other hand, "Biological adhesion", "Cell adhesion", and "Cell-cell adhesion" showed higher DMGs involved in the specific pathway (Fig. 5A). As for the CC term, these genes showed enrichment in "Integral", and "Intrinsic" component of plasma membrane (Fig. 5B and Supplementary Table 10). Besides, the MF term indicated enrichment predominantly at "Scaffold protein binding", "Calcium ion binding", and "Metal ion binding"; whereas the most genes were in the "Cation binding", and "Metal ion binding" (Fig. 5C and Supplementary Table 11). The most hypo-methylated gene was *CCND3* (q value 4.41E-09), and the highest hyper-methylated gene was *RNF166* (q value 3.86E-08) for ACS-EVs *vs* HS-EVs, whereas *AEBP2* (q value 4.32E-05) and *TESC* (q value 1.01E-03) were the most hypo-methylated and hyper-methylated genes respectively, for ACS-EVs *vs* untreated PBMCs. Notable, it was reported that *CCND3* was involved in arterial endothelial dysfunction leading to atherosclerotic lesions formation in human through SASH1 expression [37], other than into lineage differentiation and cell cycle regulation of cardiac cells [38]. For the second gene, instead there isn't evidence of potential link between *RNF166* and CVD, although *RNF166* represent a

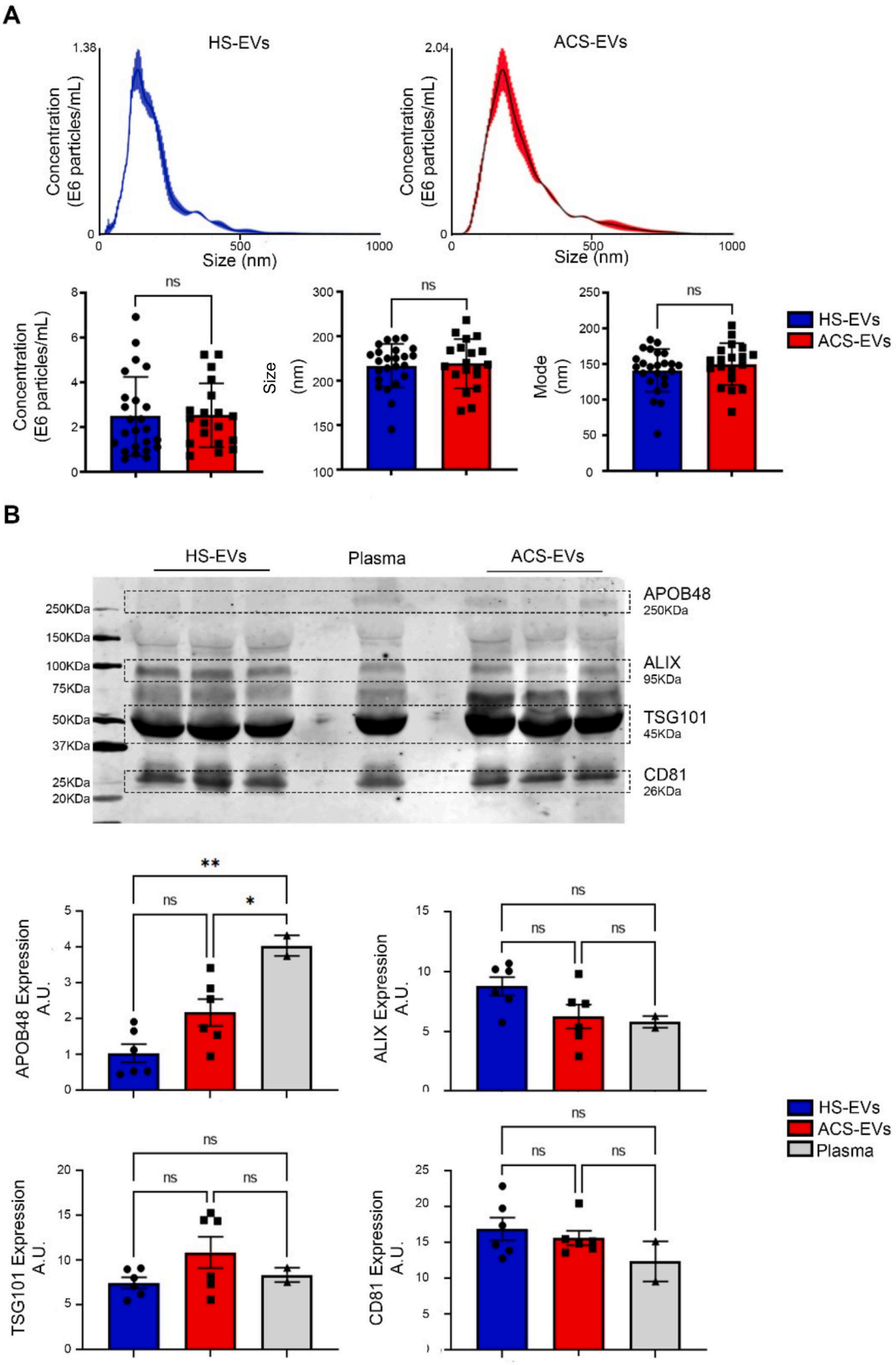

Fig. 1. Characterization of extracellular vesicles (EVs) ACS- and HS-derived.
(A) Extracellular Vesicle (EV) size and concentration detected by the nanoparticle tracking analysis in 3–5 independent samples per each group. (B) Western blots with the indicated antibodies: ALIX, TSG101, and CD81 as EV markers and APO B48 as purity control. The corresponding densitometric quantification of changes in the EV content of the indicated proteins in the experimental conditions is also represented. Equal amounts of proteins were loaded per lane. Experiments were performed at least in triplicate. The data are mean ± SE.

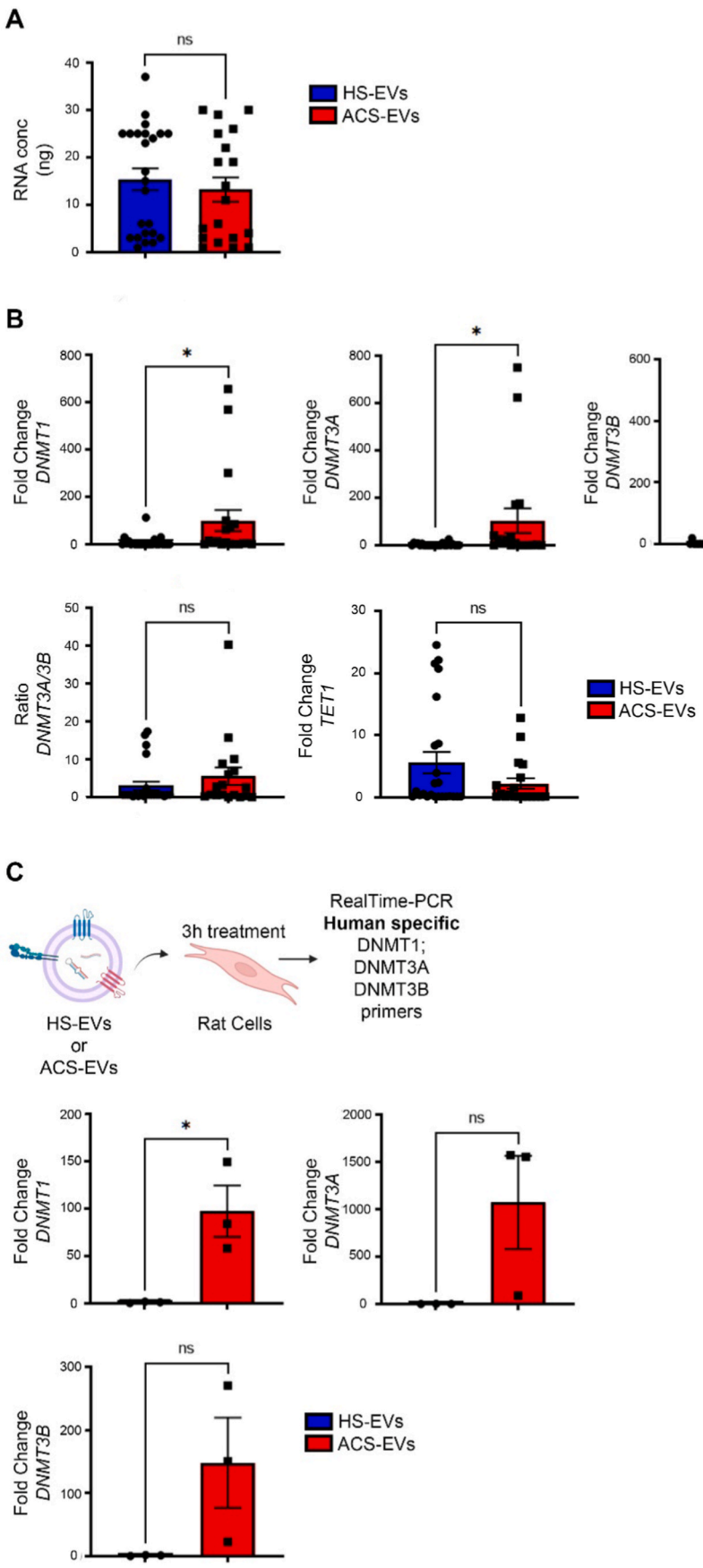

Fig. 2. EV-derived mRNA DNMTs and TETs. (A) EVs RNA content in each group. (B) Real Time-PCR for DNMTs and TET1 expression in HS-EVs and ACS-EVs. Data are expressed as fold change (FC) of the HS-EVs mRNA content. (C) Schematic illustration of the experimental setting. Real Time-PCR for DNMT1, DNMT3A and DNMT3B on rat cardiac fibroblasts treated with HS-EVs and ACS-EVs. Data are expressed as FC of the HS-EVs mRNA content. The data are mean ± SE.

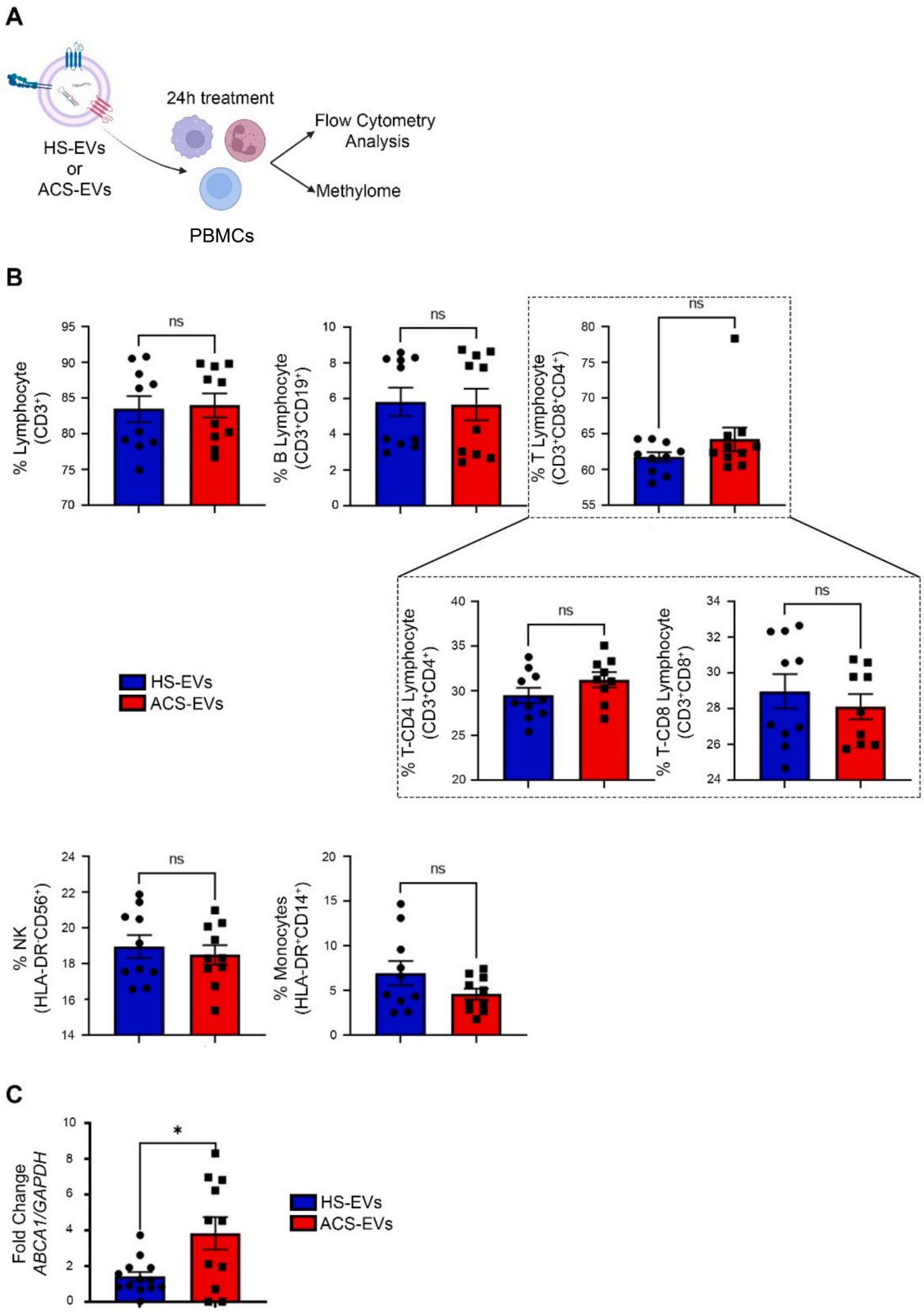

Fig. 3. PBMCs analysis.
(A) Schematic illustration of the experimental setting. (B) Flow cytometry analysis of PBMCs treated with HS- and ACS-EVs. (C) Real Time-PCR for ABCA1 expression on PBMCs treated with ACS- and HS-EVs.

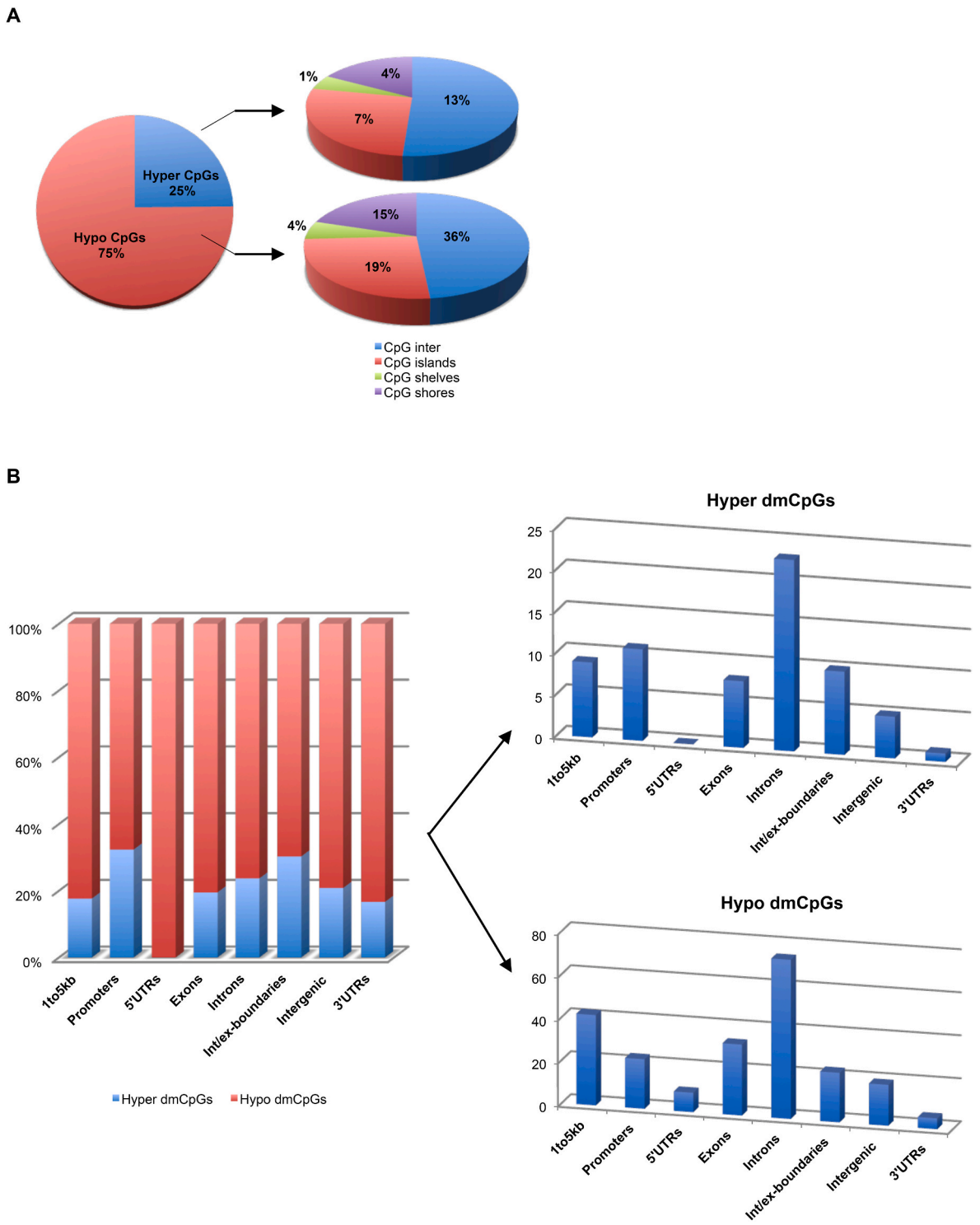

Fig. 4. PBMC methylome analysis after ACS-EVs treatment.
DNA methylation patterns identified by RRBS approach in ACS- *vs* HS-EVs treated PBMCs. (A) Distribution of differential methylated CpGs (dmCpGs) types. (B) Distribution of hyper- and hypo-methylated CpGs located at different genomic regions.

potential novel target gene for thyroid hormone receptor a1, including a genomic sequence coding for 3′-UTR [39]. To further analyze the DMG-enriched pathways, PANTHER pathway analysis was subsequently conducted. As shown in Fig. 5D, it mostly covered the "Cadherin signaling pathway" (P00012), "Wnt signaling pathway" (P00057), "Angiogenesis" (P00005), "CCKR signaling map" (P06959), "Integrin signaling pathway" (P00034), "PI3 kinase pathway" (P00048), "NOTCH signaling pathway" (P00045), and "Gonadotropin-releasing hormone receptor pathway" (P06664) (Supplementary Table 12). Specifically, a total of 40 genes were found, of which 37 hypo-methylated and 3 hyper-methylated (*SLC6A18, TF, SMURF1*). Different genes, like *PCDHA8, PCDHA1, PCDHA7, PCDHGB2, PCDHA10, PCDHA2, PCDHA4, PCDHA9, PCDHGA5, PCDHGA2, PCDHA12, PCDHA6, PCDHA11, PCDHA5, PCDHGA3, PCDHA3, PCDHGA1, PCDHGB1, PCDHGB3, SRC, CDC42*, which were always hypo-methylated, were present in multiple pathways.

(caption on next page)

Fig. 5. Gene ontology (GO) enrichment and PANTHER pathway analysis of the DMGs dataset after PBMCs treatment with ACS-EVs and PPI network analysis. GO enrichment was evaluated at three different levels: (A) biological process (BP), (B) cellular component (CC), and (C) molecular function (MF) by ShinyGO. The colour gradient represents adjusted *p*-values and the differences in bubble size correlate with the enrichment factor. (D) PANTHER pathway analysis covering signalling cathegories, ranked by fold enrichment following analysis of all DMGs PBMC-associated treatment. Only the categories showing a statistically significant enrichment are depicted. (E) The second order analysis in order to identify DMGs, which could interact with atherosclerotic genes. Each node represents all the proteins produced by a single, protein-coding gene locus. Filled nodes indicate protein with a known or predicted 3D structure; empty nodes indicate proteins of unknown 3D structure. Edges represent protein-protein associations that can be classified as known and predicted interactions, and others.

3.6. PPI network construction of DMGs

STRING database has been explored in order to assemble, predict and evaluate protein-protein association information and co-expression interactions/functions of DMGs that exhibited a significantly different methylation level, including both hyper- and hypo-methylates [40–42]. The data output provided a network with 122 nodes and 70 edges, with a PPI enrichment p value of 5.71E-06 (mean node grade of 1.15 and mean local clustering coefficient of 0.36) (Supplementary Figure 3). The most enriched networks collect terms included in the main pathways related to the mechanism of "cell adhesion" and "cell-cell adhesion", as emerged in the first level GO analysis. In order to find out whether the "molecular signals" conveyed by ACS-derived EVs produce intracellular changes, which underlie CVD, we focused our attention on the more enriched network (Fig. 5E). The central assumption of the second order analysis was to identify one or more DMGs that could interact with known genes related to atherosclerosis and, therefore, could also be functionally relevant for the development of ACS. Our cardiovascular sub-network was characterized by 41 nodes and 29 edges with PPI enrichment p value of 0.000101 (average node degree of 1.41 and average local clustering coefficient of 0.344), where the hub DMG was the proto-oncogene tyrosine-protein kinase Src (*SRC*) and the PPIs connected others 10 hub DMGs: Notch Receptor 1 (*NOTCH1*), Forkhead Box O3 (*FOXO3*), brain-specific angiogenesis inhibitor 1-associated protein 2 (*BAIAP2*), Cell Division Cycle 42 (*CDC42*), inhibitor of nuclear factor kappa B kinase regulatory subunit gamma (*IKBKG*), retinoid X receptor alpha (*RXRA*), diacylglycerol kinase gamma (*DGKG*), synaptophysin (*SYP*), cell adhesion molecule L1 like (*CHL1*), and SH2 domain containing adaptor protein B (*SHB*). Among all these genes, only for some (*NOTCH1, FOXO3, CDC42, IKBKG, RXRA, DGKG, BAIAP2*) there is molecular evidence of their involvement in CVD, such as hypertension, cardiac remodelling, vascular smooth muscle cells (VSMCs) and endothelial cell (ECs) differentiation [43–53].

On the other hand, for the following genes: *SYP, CHL1*, and *SHB* there are still no evidence in the literature about a possible role in CVDs. In addition, the network analysis also revealed connections with genes, which did not have direct links with *SRC*, such as *CCND3* (as reported in the "Gene Functional Enrichment Analysis" section), and *STIP1*

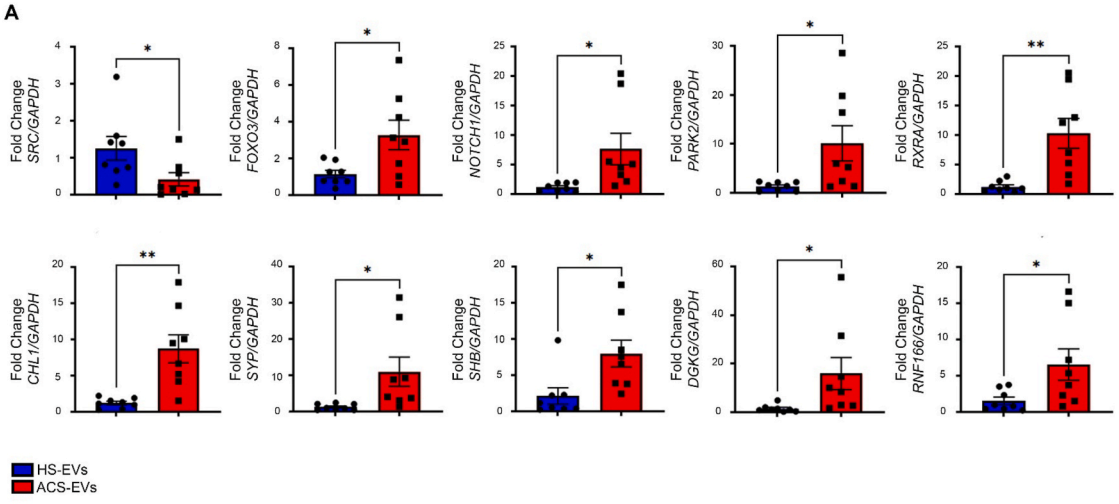

B

Spearman Rho Correlations		*DNMT1*	*DNMT3A*	*DNMT3B*	*DNMT3A/3B*	*ABCA1*	*SRC*	*FOXO3*	*NOTCH1*	*PARK2*	RXRA	CHL1	SYP	SHB	DGKG	RNF166
Age (years)	Rho	-0.331	-0.356	0.003	-0.284	-0,633*	-0.263	0.120	-0.287	-0.359	-0.407	-0.299	-0.299	-0.204	0.024	-0.156
	P- value	0.166	0.135	0.991	0.239	**0.036**	0.528	0.778	0.490	0.382	0.317	0.471	0.471	0.629	0.955	0.713
HR (bpm)	Rho	-0.067	-0.015	0.001	0.056	-0.300	0.434	0.036	0.506	0.386	0.386	0.169	0.494	0.024	0.277	0.458
	P- value	0.784	0.952	0.996	0.820	0.371	0.283	0.932	0.201	0.346	0.346	0.690	0.213	0.955	0.506	0.254
SBP (mmHg)	Rho	-0.158	-0.168	-0.045	-0.193	0.167	0.072	-0.659	0.000	-0.096	-0.108	-0.072	-0.144	0.240	-0.144	-0.395
	P- value	0.520	0.492	0.856	0.429	0.624	0.866	0.076	1.000	0.821	0.799	0.866	0.734	0.568	0.734	0.333
DBP (mmHg)	Rho	0.120	0.136	0.103	-0.024	0.413	0.184	-0.651	-0.086	-0.110	-0.135	-0.123	-0.196	0.000	-0.246	-0.405
	P- value	0.626	0.579	0.675	0.922	0.206	0.662	0.081	0.840	0.795	0.750	0.772	0.641	1.000	0.558	0.319
Total cholesterol (mg/dL)	Rho	0.221	0.071	-0.203	0.219	0.345	-0.333	-0.571	-0.667	-0.190	-0.357	-0.214	-0.643	-0.381	-0,762*	-0,714*
	P- value	0.363	0.772	0.404	0.367	0.298	0.420	0.139	0.071	0.651	0.385	0.610	0.086	0.352	**0.028**	**0.047**
LDL (mg/dL)	Rho	0.309	0.166	-0.065	0.251	0.145	-0.190	-0.571	-0.690	-0.548	-0.690	-0.548	-0.548	-0.595	-0.690	-0.667
	P- value	0.198	0.496	0.791	0.301	0.670	0.651	0.139	0.058	0.160	0.058	0.160	0.160	0.120	0.058	0.071
HDL (mg/dL)	Rho	-0.183	-0.128	-0.424	0.169	0.364	-0.168	-0.024	0.455	0,934**	0,874**	0,850**	0.240	0.467	0.036	0.144
	P- value	0.454	0.600	0.071	0.489	0.272	0.691	0.955	0.257	**0.001**	**0.005**	**0.007**	0.568	0.243	0.933	0.734
Triglycerides (mg/dL)	Rho	0.235	0,533*	-0.148	0,654**	0.445	-0.119	-0.143	-0.524	-0.429	-0.476	-0.381	-0.310	-0.476	-0.476	-0.333
	P- value	0.332	**0.019**	0.546	**0.002**	0.170	0.779	0.736	0.183	0.289	0.233	0.352	0.456	0.233	0.233	0.420
Glicemia (mg/dL)	Rho	-0.115	0.089	-0.149	0.179	-0.182	0.000	0.524	-0.190	-0.238	-0.167	-0.238	-0.024	-0.095	0.119	0.262
	P- value	0.639	0.717	0.543	0.463	0.593	1.000	0.183	0.651	0.570	0.693	0.570	0.955	0.823	0.779	0.531
TnI (ng/L)	Rho	-0.109	-0.248	-0.203	-0.126	-0.327	0.452	0.167	-0.262	-0,738*	-0.595	-0.690	-0.190	-0.286	0.214	0.048
	P- value	0.657	0.307	0.404	0.606	0.326	0.260	0.693	0.531	**0.037**	0.120	0.058	0.651	0.493	0.610	0.911
CK-MB (U/L)	Rho	-0.009	-0.020	-0.156	0.069	-0.264	0.357	0.000	-0.524	-0.619	-0.619	-0,714*	-0.429	-0.690	-0.167	-0.143
	P- value	0.972	0.937	0.524	0.778	0.433	0.385	1.000	0.183	0.102	0.102	**0.047**	0.289	0.058	0.693	0.736

Fig. 6. Revised. Expression validation of DMGs modified by EV-ACS treatment.
(A) RealTime-PCR for *SRC, FOXO3, NOTCH1, PARK2, RXRA, CHL1, SYP, SHB, DGKG* and *RNF166* on PBMCs treated with HS- and ACS-EVs. (B) Correlation between gene expression of PBMCs treated with EV-ACS derived and clinical parameters of the patients.

homology and U-box-containing protein 1 (*STUB1*), which are already connected with CVD [54]. Indeed, the E3 ubiquitin ligase *STUB1* down-regulation was detected during heart failure with preserved ejection fraction (HFpEF), governing *FOXO1* stability in cardiomyocytes [54].

Finally, a new target appeared in the network, Parkin is a RING domain-containing E3 ubiquitin ligase (*PARK2*), which did not emerge from the selected list of 141 significantly differentially methylated, but which is involved in atherosclerosis [55]. Genetic studies indicate that *PARK2* is essential for heart repair, suggesting a requirement for mitochondrial quality control in regenerating myocardium [56]. In our opinion, all these genes could be directly or indirectly altered in ACS patients by EV signals.

3.7. Validation of hub gene expression by ACS-EVS treatment

To evaluate the results obtained with the RRBS method, we validated a list of target genes, including the DMGs with the highest level of methylation difference, such as *RNF166* as hyper- and *CCND3* hypo-methylated genes; and the top 20 DMGs predicted by PPI network, which were shown in Fig. 5E (*NOTCH1, FOXO3, CDC42, IKBKG, RXRA, DGKG, STUB1, SRC, PARK2, ASAP1, PCDHGA3, CHL1, SYP, SHB, PRKD1, BAIAP2, IL4l1, ZFPM1, SMURF1 and TSPAN4*), through RT-PCR on PBMCs treated with ACS- and HS-derived EVs. Among all the validated genes we found significant altered expression between PBMCs treated with ACS- and HS-EVs of *SRC, FOXO3, PARK2, SYP, SHB, DGKG, RNF166* ($p < 0.05$) and *RXRA, CHCL1* ($p < 0.01$) (Fig. 6A). Interestingly, absolute gene expression of *PARK2, RXRA, CHCL1, DGKG* and *RNF166* in PBMCs treated with ACS-EVs were also correlated with clinical parameters of the patients (Fig. 6A and B).

4. Discussion

The main findings of our study are that 1) plasma ACS-derived EVs carry functional DNMTs mRNAs and 2) DNMTs in EVs plasma of ACS patients are significantly overexpressed compared to HS ($p < 0.05$) (Fig. 2B). As reported, DNA methylation in humans is basically performed by three functional DNMTs; constitutive DNMT1 is responsible for baseline methylation based on hemimethylated DNA, while DNMT3A and DNMT3B are responsible for *de novo* methylation in the absence of hemimethylated DNA [57]. Therefore, DNMT1, DNMT3A and DNMT3B regulate gene expression by modifying DNA methylation and altering the transcription mechanism. Here we showed, for the first time, the presence of DNMTs mRNAs into ACS patients derived EVs. Considering that EVs are capable of directly transferring RNA to target cells [58], we investigated the possible role of ACS-EVs in the modulation of specific genes in target cells through epigenetic-sensitive modifications. To determine a pathological correlation of known circulating *de novo* methylators *vs* maintenance methylators in ACS patients, we investigated PBMC-derived methylome after ACS- *vs* HS-EVs treatment and validated mRNA expression of target genes, which were found to be modulated by circulating EVs in response to ACS. We analyzed the hub genes derived by epigenome-wide analysis in circulating cells of ACS patients and HS [23]. First, we observed that ACS-derived EVs induced *ABCA1* significant gene expression alteration in healthy PBMCs (Fig. 3C), in accordance with the modulation showed in our previous study on PBMCs from ACS patients, suggesting that EVs has a fundamental role in gene expression alteration regulation [23]. In addition, ACS-EVs induced a targeted modulation of *SRC*, *NOTCH1, FOXO3, BAIAP2, CDC42, IKBKG, RXRA, DGKG, SYP, CHL1,* and *SHB* genes. As previously reported, *NOTCH1, FOXO3, CDC42, IKBKG, RXRA, DGKG, SRC* genes are already involved in CVDs [41,42,44–47,51,53,59,62]. In particular, we observed that *FOXO3* showed significant hypo-methylated CpGs in the 5′UTR and exon regions (start108561195 - end108561194) (q value 2.99E-04) and a corresponding significant transcript overexpression in PBMC ACS-EVs treated ($p < 0.05$). The same trend was also evidenced for *NOTCH1*, and *RXRA*, which showed significant intronic hypo-methylation (start136522549 - end136522548 and start134341611 - end134341610, respectively) (q value 1.69E-03 and 2.12E-03) and significant high expression levels in target cells ($p < 0.05$) (Fig. 6A). Some studies reported that reduced levels of *FOXO3* correlates with atherosclerosis, vascular calcification, vascular aging-related heart disease, and primary hypertension; *NOTCH1* mutations or its down-regulation affect cardiac abnormalities in genetically engineered mice and humans, other than abnormalities of the aortic arch, and *RXRA* is considered to play an important role in the pathogenesis of tetralogy of Fallot other than in lipid metabolism and dilated cardiomyopathy [41,42,44,60–64]. Furthermore, *SRC*, the hub gene of the predicted enriched sub-network, reported significant hypo-methylated CpGs in the intronic region (q value 3.17E-03) and most significant overexpression in its transcript after ACS-EVs treatment ($p < 0.05$). Interestingly, our study-design identified novel target genes, which may be involved in the onset and progression of ACS. For the first time, ACS-EVs induced significant activation of *SYP*, *CHL1* and *SHB* genes ($p < 0.05$), for which the literature never showed a CVDs involvement. Considering the above evidence and in according with previous studies, our findings underlie the potential stress-response role of ACS-EVs [65–69]. Our hypothesis that circulating EVs from ACS patients are secreted in response to cell damage and carry stress-response effects molecules is also supported by the observed correlations between clinical parameters, such as serum TnT and total cholesterol levels and changes in gene expression by PBMCs from the same patients upon EV-ACS treatment (Fig. 6B). Taken together, these findings suggest a potential "novel" role for circulating EVs as epigenetic regulatory factors. These results improve our understanding of the role of EVs in the epigenetic regulation of target cells and the development of CVD.

Financial support

This study was funded by: PRIN2017F8ZB89 from the Italian Ministry of University and Research (MIUR) (Claudio Napoli) and Ricerca Corrente (RC) 2019 from the Italian Ministry of Health (Claudio Napoli); competitive Research Grant "VALERE: Vanvitelli Project 2020" (Concetta Schiano) from the Italian Ministry of University and Research (MUR); Swiss National Science Foundation grant no. 169194 (Giuseppe Vassalli). Swiss Heart Foundation no. FF21017 (Carolina Balbi).

Declaration of competing interest

The authors declare that they have no known competing financial interests or personal relationships that could have appeared to influence the work reported in this paper.

CRediT authorship contribution statement

Concetta Schiano: Conceptualization, Data curation, Formal analysis, Investigation, Project administration, Resources, Software, Supervision, Validation, Visualization. **Carolina Balbi:** Conceptualization, Data curation, Formal analysis, Funding acquisition, Investigation, Project administration, Resources, Software, Supervision, Validation, Visualization, Writing – original draft. **Jacopo Burrello:** Methodology. **Antonio Ruocco:** Methodology. **Teresa Infante:** Methodology. **Carmela Fiorito:** Methodology. **Stefano Panella:** Methodology. **Lucio Barile:** Writing – review & editing. **Ciro Mauro:** Funding acquisition, Project administration, Resources, Software, Supervision, Validation, Visualization, Writing – review & editing. **Giuseppe Vassalli:** Funding acquisition, Project administration, Resources, Software, Supervision, Validation, Visualization, Writing – review & editing. **Claudio Napoli:** Funding acquisition, Writing – review & editing.

Appendix A. Supplementary data

Supplementary data to this article can be found online at https://doi.org/10.1016/j.atherosclerosis.2022.06.1026.

References

[1] T. Infante, C. Cavaliere, B. Punzo, et al., Radiogenomics and artificial intelligence approaches applied to cardiac computed tomography angiography and cardiac magnetic resonance for precision medicine in coronary heart disease: a systematic review, Circ. Cardiovasc. Image 14 (2021) 1133–1146, https://doi.org/10.1161/CIRCIMAGING.121.013025.

[2] C. Théry, K.W. Witwer, E. Aikawa, et al., Minimal information for studies of extracellular vesicles 2018 (MISEV2018): a position statement of the International Society for Extracellular Vesicles and update of the MISEV2014 guidelines, J. Extracell. Vesicles 7 (2018), 1535750, https://doi.org/10.1080/20013078.2018.1535750.

[3] C. Balbi, Editorial: transverse aortic constriction-induced heart failure leads to increased levels of circulating microparticles, Int. J. Cardiol. 348 (2022) 109–110, https://doi.org/10.1016/j.ijcard.2021.12.003.

[4] G. Benincasa, G. Mansueto, C. Napoli, Fluid-based assays and precision medicine of cardiovascular diseases: the 'hope' for Pandora's box? J. Clin. Pathol. 72 (2019) 785–799, https://doi.org/10.1136/jclinpath-2019-206178.

[5] C. Arenaccio, M. Federico, The multifaceted functions of exosomes in health and disease: an overview, Adv. Exp. Med. Biol. 998 (2017) 3–19, https://doi.org/10.1007/978-981-10-4397-0_1.

[6] C. Balbi, K. Lodder, A. Costa, et al., Reactivating endogenous mechanisms of cardiac regeneration via paracrine boosting using the human amniotic fluid stem cell secretome, Int. J. Cardiol. 287 (2019) 87–95, https://doi.org/10.1016/j.ijcard.2019.04.011.

[7] C. Balbi, M. Piccoli, L. Barile, et al., First characterization of human amniotic fluid stem cell extracellular vesicles as a powerful paracrine tool endowed with regenerative potential, Stem Cells Transl. Med. 6 (2017) 1340–1355, https://doi.org/10.1002/sctm.16-0297.

[8] C. Balbi, J. Burrello, S. Bolis, et al., Circulating extracellular vesicles are endowed with enhanced procoagulant activity in SARS-CoV-2 infection, EBioMedicine 67 (2021), 103369, https://doi.org/10.1016/j.ebiom.2021.103369.

[9] C.S. Zhang, K. Shao, C.W. Liu, Li, et al., Hypoxic preconditioning BMSCs-exosomes inhibit cardiomyocyte apoptosis after acute myocardial infarction by upregulating microRNA-24, Eur. Rev. Med. Pharmacol. Sci. 23 (2019) 6691–6699, https://doi.org/10.26355/eurrev_201908_18560.

[10] L. Barile, E. Cervio, V. Lionetti, et al., Cardioprotection by cardiac progenitor cell-secreted exosomes: role of pregnancy-associated plasma protein-A, Cardiovasc. Res. 114 (2018) 992–1005, https://doi.org/10.1093/cvr/cvy055.

[11] L. Barile, V. Lionetti, E. Cervio, et al., Extracellular vesicles from human cardiac progenitor cells inhibit cardiomyocyte apoptosis and improve cardiac function after myocardial infarction, Cardiovasc. Res. 103 (2014) 530–541, https://doi.org/10.1093/cvr/cvu167.

[12] E.A. Mol, M.J. Goumans, J.P.G. Sluijter, Cardiac progenitor-cell derived exosomes as cell-free therapeutic for cardiac repair, Adv. Exp. Med. Biol. 998 (2017) 207–219, https://doi.org/10.1007/978-981-10-4397-0_14.

[13] J. Xiao, Y. Pan, X.H. Li, et al., Cardiac progenitor cell-derived exosomes prevent cardiomyocytes apoptosis through exosomal miR-21 by targeting PDCD4, Cell Death Dis. 7 (2016) e2277, https://doi.org/10.1038/cddis.2016.181.

[14] J. Burrello, A. Burrello, E. Vacchi, et al., Supervised and unsupervised learning to define the cardiovascular risk of patients according to an extracellular vesicle molecular signature, Transl. Res. 244 (2022) 114–125, https://doi.org/10.1016/j.trsl.2022.02.005.

[15] J. Burrello, G. Bianco, A. Burrello, et al., Extracellular vesicle surface markers as a diagnostic tool in transient ischemic attacks, Stroke 52 (2021) 3335–3347, https://doi.org/10.1161/STROKEAHA.120.033170.

[16] M. Gartz, J.L. Strande, Examining the paracrine effects of exosomes in cardiovascular disease and repair, J. Am. Heart Assoc. 7 (2018), e007954, https://doi.org/10.1161/JAHA.117.007954.

[17] Y. Pan, G. Liu, F. Zhou, et al., DNA methylation profiles in cancer diagnosis and therapeutics, Clin. Exp. Med. 18 (2018) 1–14, https://doi.org/10.1007/s10238-017-0467-0.

[18] A. Zemach, I.E. McDaniel, P. Silva, et al., Genome-wide evolutionary analysis of eukaryotic DNA methylation, Science 328 (2010) 916–919, https://doi.org/10.1126/science.1186366.

[19] J. Zhuang, P. Luan, H. Li, et al., The yin-yang dynamics of DNA methylation is the key regulator for smooth muscle cell phenotype switch and vascular remodeling, Arterioscler. Thromb. Vasc. Biol. 37 (2017) 84–97, https://doi.org/10.1161/ATVBAHA.116.307923.

[20] C.D. Allis, T. Jenuwein, The molecular hallmarks of epigenetic control, Nat. Rev. Genet. 17 (2016) 487–500, https://doi.org/10.1038/nrg.2016.59.

[21] X. Wu, Y. Zhang, TET-mediated active DNA demethylation: mechanism, function and beyond, Nat. Rev. Genet. 18 (2017) 517–534, https://doi.org/10.1038/nrg.2017.33.

[22] P.A. Ginno, D. Gaidatzis, A. Feldmann, et al., A genome-scale map of DNA methylation turnover identifies site-specific dependencies of DNMT and TET activity, Nat. Commun. 11 (2020) 2680, https://doi.org/10.1038/s41467-020-16354-x.

[23] T. Infante, M. Franzese, A. Ruocco, et al., ABCA1, TCF7, NFATC1, PRKCZ, and PDGFA DNA methylation as potential epigenetic-sensitive targets in acute coronary syndrome via network analysis, Epigenetics 17 (2022) 547–563, https://doi.org/10.1080/15592294.2021.1939481.

[24] F. Cacciatore, G. Bruzzese, P. Abete, et al., Maternal hypercholesterolaemia during pregnancy affects severity of myocardial infarction in young adults, Eur J Prev Cardiol 29 (2022) 758–765, https://doi.org/10.1093/eurjpc/zwab152.

[25] C. Schiano, G. Benincasa, T. Infante, et al., Integrated analysis of DNA methylation profile of HLA-G gene and imaging in coronary heart disease: pilot study, PLoS One 15 (2020), e0236951, https://doi.org/10.1371/journal.pone.0236951.

[26] C. Schiano, G. Benincasa, M. Franzese, et al., Epigenetic-sensitive pathways in personalized therapy of major cardiovascular diseases, Pharmacol. Ther. 210 (2020), 107514, https://doi.org/10.1016/j.pharmthera.2020.107514.

[27] T. Infante, E. Forte, B. Punzo, et al., Correlation of circulating miR-765, miR-93-5p, and miR-433-3p to obstructive coronary heart disease evaluated by cardiac computed tomography, Am. J. Cardiol. 124 (2019) 176–182, https://doi.org/10.1016/j.amjcard.2019.04.016.

[28] F. de Nigris, F. Cacciatore, F.P. Mancini, et al., Epigenetic hallmarks of fetal early atherosclerotic lesions in humans, JAMA Cardiol. 3 (2018) 1184–1191, https://doi.org/10.1001/jamacardio.2018.3546.

[29] C. Schiano, M.T. Vietri, V. Grimaldi, et al., Epigenetic-related therapeutic challenges in cardiovascular disease, Trends Pharmacol. Sci. 36 (2015) 226–235, https://doi.org/10.1016/j.tips.2015.02.005.

[30] C. Napoli, V. Crudele, A. Soricelli, et al., Primary prevention of atherosclerosis: a clinical challenge for the reversal of epigenetic mechanisms? Circulation 125 (2012) 2363–2373, https://doi.org/10.1161/CIRCULATIONAHA.111.085787.

[31] C. Napoli, L.O. Lerman, Involvement of oxidation-sensitive mechanisms in the cardiovascular effects of hypercholesterolemia, Mayo Clin. Proc. 76 (2001) 619–631, https://doi.org/10.4065/76.6.619.

[32] S.X. Ge, D. Jung, R. Yao, ShinyGO: a graphical gene-set enrichment tool for animals and plants, Bioinformatics 36 (2020) 2628–2629, https://doi.org/10.1093/bioinformatics/btz931.

[33] H. Mi, D. Ebert, A. Muruganujan, et al., PANTHER version 16: a revised family classification, tree-based classification tool, enhancer regions and extensive API, Nucleic Acids Res. 49 (2021) D394–D403, https://doi.org/10.1093/nar/gkaa1106.

[34] C. von Mering, M. Huynen, D. Jaeggi, et al., STRING: a database of predicted functional associations between proteins, Nucleic Acids Res. 31 (2003) 258–261, https://doi.org/10.1093/nar/gkg034.

[35] J. Burrello, S. Bolis, C. Balbi, et al., An extracellular vesicle epitope profile is associated with acute myocardial infarction, J. Cell Mol. Med. 24 (2020) 9945–9957, https://doi.org/10.1111/jcmm.15594.

[36] T. Infante, E. Forte, C. Schiano, et al., Evidence of association of circulating epigenetic-sensitive biomarkers with suspected coronary heart disease evaluated by Cardiac Computed Tomography, PLoS One 14 (2019), e0210909, https://doi.org/10.1371/journal.pone.0210909.

[37] H. Weidmann, Z. Touat-Hamici, H. Durand, et al., SASH1, a new potential link between smoking and atherosclerosis, Atherosclerosis 242 (2015) 571–579, https://doi.org/10.1016/j.atherosclerosis.2015.08.013.

[38] I. Lei, S. Tian, V. Chen, et al., SWI/SNF component BAF250a coordinates OCT4 and WNT signaling pathway to control cardiac lineage differentiation, Front. Cell Dev. Biol. 7 (2020) 358, https://doi.org/10.3389/fcell.2019.00358.

[39] S. Dudazy-Gralla, K. Nordström, P.J. Hofmann, et al., Identification of thyroid hormone response elements in vivo using mice expressing a tagged thyroid hormone receptor α1, Biosci. Rep. 33 (2013), e00027, https://doi.org/10.1042/BSR20120124.

[40] A. Franceschini, D. Szklarczyk, S. Frankild, et al., STRING v9.1: protein-protein interaction networks, with increased coverage and integration, Nucleic Acids Res. 41 (Database issue) (2013) D808–D815, https://doi.org/10.1093/nar/gks1094.

[41] E.K. Silverman, H.H.H.W. Schmidt, E. Anastasiadou, et al., Molecular Networks in Network Medicine: Development and Applications, vol. 12, Wiley Interdiscip Rev Syst Biol Med, 2020, p. e1489, https://doi.org/10.1002/wsbm.1489.

[42] F. Sarno, G. Benincasa, M. List, et al., International Network Medicine Consortium. Clinical epigenetics settings for cancer and cardiovascular diseases: real-life applications of network medicine at the bedside, Clin. Epigenet. 13 (2021) 66, https://doi.org/10.1186/s13148-021-01047-z.

[43] L. Li, I.D. Krantz, Y. Deng, et al., Alagille syndrome is caused by mutations in human Jagged1, which encodes a ligand for Notch1, Nat. Genet. 16 (1997) 243–251, https://doi.org/10.1038/ng0797-243.

[44] Y. Zhao, Y.S. Liu, Longevity factor FOXO3: a key regulator in aging-related vascular diseases, Front Cardiovasc. Med. 8 (2021), 778674, https://doi.org/10.3389/fcvm.2021.778674.

[45] Y. Shi, L. Zhao, Y. Zhang, et al., Homocysteine promotes cardiac fibrosis by regulating the Akt/FoxO3 pathway, Ann. Transl. Med. 9 (2021) 1732, https://doi.org/10.21037/atm-21-5602.

[46] W. Lu, Y. Zhou, S. Zeng, et al., Loss of FoxO3a prevents aortic aneurysm formation through maintenance of VSMC homeostasis, Cell Death Dis. 12 (2021) 378, https://doi.org/10.1038/s41419-021-03659-y.

[47] E. Zhou, Y. Zou, C. Mao, et al., MicroRNA-221 inhibits the transition of endothelial progenitor cells to mesenchymal cells via the PTEN/FoxO3a signaling pathway, Adv. Clin. Exp. Med. 30 (2021) 1263–1270, https://doi.org/10.17219/acem/141446.

[48] K. Miyamoto, K.Y. Araki, K. Naka, et al., Foxo3a is essential for maintenance of the hematopoietic stem cell pool, Cell Stem Cell 1 (2007) 101–112, https://doi.org/10.1016/j.stem.2007.02.001.

[49] D. Liu, X. Tian, Y. Liu, et al., CREG ameliorates the phenotypic switching of cardiac fibroblasts after myocardial infarction via modulation of CDC42, Cell Death Dis. 12 (2021) 355, https://doi.org/10.1038/s41419-021-03623-w.
[50] S. Gao, M. Menendez, K. Kurylowicz, et al., Genomic locus proteomic screening identifies the NF-κB signaling pathway components NFκB1 and IKBKG as transcriptional regulators of Ripk3 in endothelial cells, PLoS One 16 (2021), e0253519, https://doi.org/10.1371/journal.pone.0253519.
[51] X. Ma, P. Zhu, Y. Ding, et al., Retinoid X receptor alpha is a spatiotemporally predominant therapeutic target for anthracycline-induced cardiotoxicity, Sci. Adv. 6 (2020), eaay2939, https://doi.org/10.1126/sciadv.aay2939.
[52] J. Zhang, X. Ma, H. Wang, et al., Elevated methylation of the RXRA promoter region may be responsible for its downregulated expression in the myocardium of patients with TOF, Pediatr. Res. 75 (2014) 588–594, https://doi.org/10.1038/pr.2014.17.
[53] E. Vahtola, M. Storvik, M. Louhelainen, et al., Effects of levosimendan on cardiac gene expression profile and post-infarct cardiac remodelling in diabetic Goto-Kakizaki rats, Basic Clin. Pharmacol. Toxicol. 109 (2011) 387–397, https://doi.org/10.1111/j.1742-7843.2011.00743.x.
[54] G.G. Schiattarella, F. Altamirano, S.Y. Kim, et al., Xbp1s-FoxO1 axis governs lipid accumulation and contractile performance in heart failure with preserved ejection fraction, Nat. Commun. 12 (2021) 1684, https://doi.org/10.1038/s41467-021-21931-9.
[55] J. Yang, M. Sun, R. Cheng, et al., Pitavastatin activates mitophagy to protect EPC proliferation through a calcium-dependent CAMK1-PINK1 pathway in atherosclerotic mice, Commun Biol. 5 (2022) 124, https://doi.org/10.1038/s42003-022-03081-w.
[56] J.P. Leach, T. Heallen, M. Zhang, et al., Hippo pathway deficiency reverses systolic heart failure after infarction, Nature 550 (2017) 260–264, https://doi.org/10.1038/nature24045.
[57] F. Lyko, The DNA methyltransferase family: a versatile toolkit for epigenetic regulation, Nat. Rev. Genet. 19 (2018) 81–92, https://doi.org/10.1038/nrg.2017.80.
[58] H. Valadi, K. Ekström, A. Bossios, et al., Exosome-mediated transfer of mRNAs and microRNAs is a novel mechanism of genetic exchange between cells, Nat. Cell Biol. 9 (2007) 654–659, https://doi.org/10.1038/ncb1596.
[59] Y. Zhai, J. Yang, J. Zhang, et al., Src-family protein tyrosine kinases: a promising target for treating cardiovascular diseases, Int. J. Med. Sci. 18 (2021) 1216–1224, https://doi.org/10.7150/ijms.49241.
[60] C. Napoli, E. Coscioni, F. de Nigris, et al., Emergent expansion of clinical epigenetics in patients with cardiovascular diseases, Curr. Opin. Cardiol. 36 (2021) 295–300, https://doi.org/10.1097/HCO.0000000000000843.
[61] D. Castellano-Castillo, I. Moreno-Indias, L. Sanchez-Alcoholado, et al., Altered adipose tissue DNA methylation status in metabolic syndrome: relationships between global DNA methylation and specific methylation at adipogenic, lipid metabolism and inflammatory candidate genes and metabolic variables, J. Clin. Med. 8 (2019) 87, https://doi.org/10.3390/jcm8010087.
[62] F.A. High, R. Jain, J.Z. Stoller, et al., Murine Jagged1/Notch signaling in the second heart field orchestrates Fgf8 expression and tissue-tissue interactions during outflow tract development, J. Clin. Invest. 119 (2009) 1986–1996, https://doi.org/10.1172/JCI38922.
[63] J. Zhang, Z. Zhang, D.Y. Zhang, et al., microRNA 126 inhibits the transition of endothelial progenitor cells to mesenchymal cells via the PIK3R2-PI3K/Akt signalling pathway, PLoS One 8 (2013), e83294, https://doi.org/10.1371/journal.pone.0083294.
[64] V. Subbarayan, M. Mark, N. Messadeq, et al., RXRalpha overexpression in cardiomyocytes causes dilated cardiomyopathy but fails to rescue myocardial hypoplasia in RXRalpha-null fetuses, J. Clin. Invest. 105 (2000) 387–394, https://doi.org/10.1172/JCI8150.
[65] F. Chatzopoulou, K.A. Kyritsis, C.I. Papagiannopoulos, et al., Dissecting miRNA-gene networks to map clinical utility roads of pharmacogenomics-guided therapeutic decisions in cardiovascular precision medicine, Cells 11 (2022) 607, https://doi.org/10.3390/cells11040607.
[66] E. Hergenreider, S. Heydt, K. Tréguer, et al., Atheroprotective communication between endothelial cells and smooth muscle cells through miRNAs, Nat. Cell Biol. 14 (2012) 249–256, https://doi.org/10.1038/ncb2441.
[67] A. Montecalvo, A.T. Larregina, W.J. Shufesky, et al., Mechanism of transfer of functional microRNAs between mouse dendritic cells via exosomes, Blood 119 (2012) 756–766, https://doi.org/10.1182/blood-2011-02-338004.
[68] M. Eldh, K. Ekström, H. Valadi, et al., Exosomes communicate protective messages during oxidative stress; possible role of exosomal shuttle RNA, PLoS One 5 (2010), e15353, https://doi.org/10.1371/journal.pone.0015353.
[69] R.C. Lai, F. Arslan, M.M. Lee, et al., Exosome secreted by MSC reduces myocardial ischemia/reperfusion injury, Stem Cell Res. 4 (2010) 214–222, https://doi.org/10.1016/j.scr.2009.12.003.